The 'WenSDak' project: (analysis and development) of aesthetic building integrated solar heat and power roofs

Corry de Keizer[1], Minne de Jong[1], Munish Katiyar[2], Wiep Folkerts[1], Camilo Rindt[2] and Herbert Zondag[2,3]

[1] Solar Energy Application Centre (SEAC), Eindhoven (the Netherlands), dekeizer@seac.cc

[2] Technical University Eindhoven, Eindhoven (the Netherlands)

[3] ECN, Petten (the Netherlands)

Abstract

In the Dutch WenSDak project, eight companies and three research institutes worked together on the (further) development of five concepts for integrating solar heat and power production into one roof. The performance of the ventilated PV, uncovered PVT and solar thermal collectors was evaluated in a field test and with a solar simulator indoors. In this paper, we focus on three types of uncovered PVT collectors. There is a large difference between the measured thermal performance of the three different collectors. These differences can be explained by the PVT collector design. The absorption of all PVT modules is quite good (0.9 – 0.94). A good heat conduction from the PV cells to a metal absorber leads to a high peak collector efficiency, while insulation at the back of the PVT module improves the performance at higher temperatures. Performance of some collectors can be improved by e.g. heat conducting paste, however, this is also more expensive. System simulations with PVT as part of a solar heating system are carried out in TRNSYS and will yield valuable information on the annual yield for a specific system.

Keywords: *PVT modules, PVT performance*
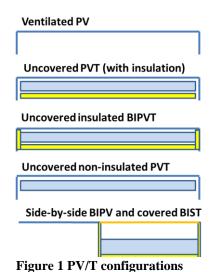
1. Introduction

European regulations are aiming at (near) zero-energy buildings in the near future. Since a large share of the energy demand in the built environment in continental Europe consists of heat, the combination of both solar heat and solar electricity production in one roof is interesting. Combining photovoltaic panels and thermal collectors in a hybrid PVT collector may result in a higher roof energy yield and a more aesthetic unified appearance of the roof.

In the Dutch 'WenSDak' project (2014-2016) several companies and research institutes work together to (further) develop five different PVT roof concepts and to evaluate their performance. The main aim is to further develop these systems and to evaluate how much these systems can contribute to a sustainable built environment. The outdoor performance as well as the indoor performance (solar simulator) are measured. The measured performance results are being used as input for annual system simulations for typical residential systems.

The PVT products developed within the WenSDak consortium can be described as follows (see also fig. 1):

- A ventilated BIPV system; heat is used for drying or for regeneration of a ground source
- An uncovered PVT system with insulation underneath
- An uncovered building integrated PVT system with insulation underneath
- A not-insulated PVT system
- A side-by-side system of a building integrated PV roof and in the same manner building integrated covered solar thermal collectors

All products are developed by one or two different companies. The uncovered PVT systems can be used in combination with a (ground source) heat pump to provide space heating or domestic hot water or for

Figure 1 PV/T configurations

preheating. The different concepts of uncovered PVT modules show a quite different performance, but also have different costs.

The aim of the project is to further develop these five different concepts and to evaluate their electrical and thermal performance. In the project we evaluate the module performance in an outdoor field test and indoors with a solar simulator. The system performance of PVT systems in different configurations will be analysed with TRNSYS simulations.

This paper focuses on the three uncovered PVT systems in the project that were developed by different project partners. The main focus will be on the field test results.

2. Field test

A field test for the three different types of uncovered PVT collectors was set up, these are:

A: a CIGS panel with clamped absorber and insulation produced by Solartech (Energiedak MEP panels)

B: c-Si PV with uninsulated absorber clamped to the back of the module, produced by GEO Holland

C: building integrated c-Si PV with in-roof absorber and insulation produced by Dimark Solar

Fig. 2: Field test with three types of uncovered PVT systems on the dummy roof

The three uncovered PVT systems were installed on the experimental outdoor field test facility of SEAC as shown in Figure 2. The following setup was installed:

• System A: 4 PVT collectors and 4 PV modules; results are shown for 4 PVT collectors, gross area of 4.4 m^2, flow rate 24 l/m^{2}h

• System B: 5 PV collectors and 3 thermal absorbers; results are shown for 2 PVT collectors, gross area of 3.3 m^2, fluid flow rate 74 l/m^{2}h

• System C: 3 PVT collectors and 3 thermal collectors; analysis of 2 PVT collectors, gross area of 3.5 m^2, flow rate 18 l/m^{2}h

The outdoor facility is located on the roof of one of the buildings of the Technical University of Eindhoven and includes a solar measurement station with which direct, diffuse and global horizontal irradiance are measured, as well as wind speed and direction and ambient temperature.

Furthermore, a thermal loop was designed and installed to allow for measurements on solar thermal collectors and PVT systems. Excess heat produced by the thermal systems is dumped in the university's aquifer. A combination of heaters, valves, chillers and control technology make sure the liquid is preconditioned to the specified temperature. The input temperature for the systems can be set between 7 and 80°C. A 25 % glycol solution is used in the PVT loop.

The collectors of each system are thermally connected in series. For each system, different flow rates are defined. However, the inlet temperature of the first collector of each system is the same. The flow rates were decided upon by the supplier of the system, to match the flows that are used in real systems. Each PVT panel is electrically connected to a DC/DC SolarEdge power optimizer. The power optimizers are in series connected to the SolarEdge DC/AC inverter. Therefore, the electrical and thermal performance of the PVT modules is measured at maximum power point for each module.

The following measurement equipment is installed:

• Meteorological measurements: Global tilted irradiance (secondary standard pyranometer), pyrgeometer, in-plane wind speed and direction, ambient temperature.

• PV performance measurements: Measurements are done at MPP (maximum power point). DC voltage and DC current (via a shunt) are measured for each PVT collector separately.

• Thermal performance measurements: input and output temperature of each collector (Pt100, 1/3B) and flow rate (Electromagnetic sensor, one per series of collectors).

• Datalogging: All sensors are connected to a Yokogawa MW100 datalogger. Data is recorded every minute and uploaded every night to a database.

The field test was running for a full year, from June 2015 to May 2016.

2.2 Evaluation of thermal performance

For analyzing the thermal efficiency, we followed the steady state analysis for unglazed collectors as described in the ISO 9806 norm [2], though there are some differences, like building integration of the PVT modules in our test site and the flow rate. The thermal efficiency (η_{th}) is calculated by Equation 1. The effective irradiance is calculated by equation 2, with the in-plane irradiance as an input. Furthermore, the pyrgeometer is used to calculate the long-wave irradiance (EL). The coefficients η_{th}, b_u, b_1 and b_2 are fitted by using a least squares method and equation 3.

$$\eta_{th} = \frac{\dot{Q}}{A_G \cdot G''} = \frac{\rho \cdot c_p \cdot \dot{V} \cdot (T_{out} - T_{in})}{A_G \cdot G''} \qquad (eq\ 1)$$

$$G'' = G_{POA} + \frac{\varepsilon}{\alpha}(E_L - \sigma T_a^4) \text{ with } \varepsilon/\alpha = 0.98 \qquad (eq\ 2)$$

$$\eta_{th} = \eta_{0,th}(1 - b_u u) - (b_1 + b_2 u)\frac{(T_m - T_a)}{G''} \qquad (eq\ 3)$$

With:
A_G Gross collector area (m^2)
b_1 heat loss coefficient (W/m^{2}K)
b_2 wind dependence of the heat loss coefficient (J/m^{3}K)
b_u collector efficiency coefficient (wind dependence) (s/m)
c_p Specific heat capacity (J/kgK)
G_{POA} Global irradiance in plane-of-array (W/m^2)

G''/G_{eff} Net irradiance (W/m^2)

T_a Ambient temperature (K)

T_m Mean collector temperature $(T_{in}+T_{out})/2$ (K)

T_{in} Input temperature (K)

T_{out} Output temperature (K)

$\dot{Q}_{th}$ Heat flow (W)

u   Wind speed (m/s)

$\dot{V}$ Volume flow (l/s)

α   Solar absorptance (%)

ε   Hemispherical emittance (%)

$\eta_{0,th}$ Peak collector efficiency (η_{th} at $T_m = T_a$)

η_{th} Thermal collector efficiency, with reference to T_m

ρ   Density (kg/l)

σ   Stefan-Boltzmann constant (W/m^{2}K^4)

3.   Results of the field test

3.1   Introduction

PVT collectors produce both heat and power. The energy yield depends on different factors, of which the most important factors are: Irradiance, ambient temperature, average fluid temperature and wind speed. Figures 3a and 3b show the produced power (heat and electricity) in W/m^2 for the three collector types. We chose two sunny days with a low (7°C) and a high (35°C) inlet temperature in summer 2015.

Irradiance in the plane-of-array is shown in green. The thermal heat is depicted by continuous lines, while in the dotted lines the electrical power is added. System B (red) does not have any insulation at the back and therefore acts as a heat exchanger at night and produces heat in Figure 3b, when the ambient temperature is higher than the collector temperature. While the PV yield is in a similar range on the two days, the thermal yield depends largely on the inlet temperature of the water.

Please note, that the average collector temperature is very different for the different collectors. System C operates at higher temperatures and therefore, produces more useful heat. System A and C perform better at higher temperatures due to the insulation at the back.
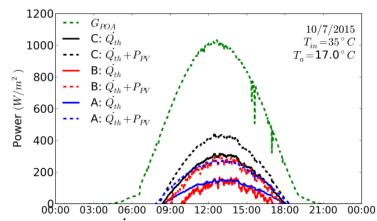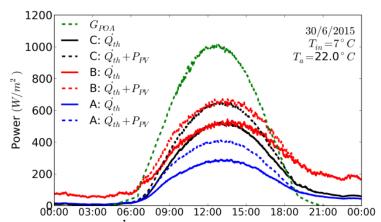

Figure 3a: Thermal (continuous lines, $\dot{Q}_{th}$) and additional electrical power output (dashed lines, $\dot{Q}_{th}+P_{PV}$) per m^2 for a day with a fluid input temperature of 35°C. In-plane irradiance (G_{POA}) is shown in green.

Figure 3b: Thermal (continuous lines, $\dot{Q}_{th}$) and additional electrical power output (dashed lines, $\dot{Q}_{th}+P_{PV}$) per m^2 for a day with a fluid input temperature of 7°C. In-plane irradiance (G_{POA}) is shown in green.

3.2   Thermal performance

The thermal efficiency is calculated based on measured data for a one year period from June 2015 to May 2016. The absorption factors of the different PVT panels were measured by ECN with an integrating sphere and was between 0.90 and 0.94 for the different panels. The emission is approximately 0.9.

The thermal collector efficiency curves for collector A, B and C are shown in Figure 4 for a wind speed of 0 and 3 m/s, with the PV in MPP. The PV efficiency (12-14%) is additional. The collectors show very different performance features. Collector C performs the best of the three measured collectors. The other collectors can also perform well in system configurations that have a low demand temperature. E.g. systems that are connected to a ground-source heat pump, often operate below ambient temperature.
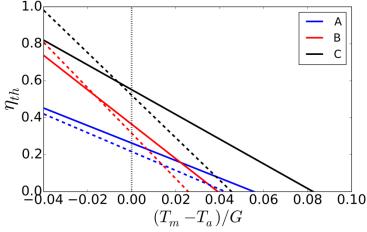

Figure 4: Collector curve for PVT collector A, B and C with a wind speed of 0 (solid) and 3 m/s (dashed), based on measured data from June 2015 to May 2016, with PV operational and measured in MPP.
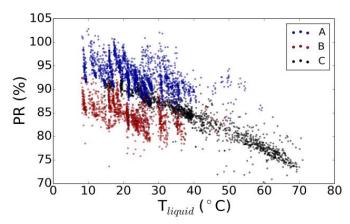
Figure 5: Correlation between the DC performance ratio and the average fluid temperature (15 minute averages, irradiance >900 W/m^2).

3.3   Overall performance

The electric performance of PVT modules is influenced by the thermal part. Figure 5 shows the correlation of the DC PV performance ratio (PR) on the average fluid temperature of the PVT collectors for days with high irradiance. It shows that the heat conduction between the PV cells and the thermal absorber of PVT collector C is good, the PR reduces with higher liquid temperatures. The mean fluid temperature is one of the main drivers of the PR for collector C. It also shows that the heat conduction between the PV cells and the fluid for systems A and B is not very good.

Figure 6a shows the correlation between the DC PV performance ratio, the ambient temperature and the average liquid temperature for the four Energiedak (system A) PVT collectors. Figure 6b shows that for the four Energiedak PV panels. At a closer look, it is clear that especially at higher ambient temperatures and lower fluid temperatures, the performance ratio for the PVT collectors is slightly higher.
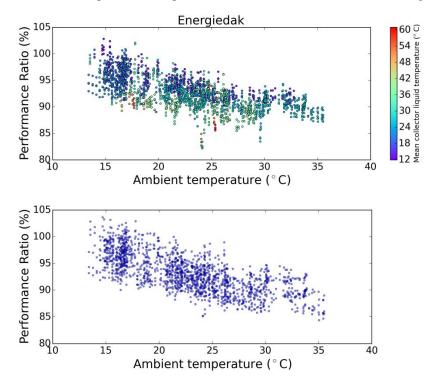

Figure 6a) Four PVT modules: Correlation between DC PV performance ratio, ambient temperature and average collector liquid temperature of system A PVT modules at G>900 W/m^2, 6b) PV only modules: correlation between DC PV performance ratio and ambient temperature at G>900 W/m^2.

The coefficients and the average electrical efficiency for all collectors are shown in Table I.

Table 1: Performance indicators

Col-lector	η_{th}	b_u (s/m)	b_1 (W/m^2 K)	b_2 (J/m^{3}K)	η_{el} (DC)
A	26 %	0.06	4.7	0.1	12.2 %
B	37 %	0.04	9.3	1.0	13.8 %
C	55 %	0.02	6.7	1.6	12.7 %

The electrical average efficiency of the three uncovered PVT systems is between 12.2 and 13.8 %. The difference is partially caused by a different peak power per square meter. The thermal efficiency parameters are for a large part caused by the thermal conduction between the PV and the thermal collector together with the insulation on the back of the system. A better thermal contact leads to a higher η0, but also to higher heat loss (b1) and wind dependency of the heat loss (b2) parameters, also when the back of the panel is insulated or integrated in the roof.

4. TRNSYS simulations

One of the main aims of the project is to determine the performance of a PVT roof as part of a building installation that supplies domestic hot water and/or space heating. To this end, we set up simulations in the TRNSYS environment. We use TRNSYS to simulate the annual performance of a full-roof solar energy solution for a typical Dutch row house. Several options are considered, regarding type of PVT collector, share of PVT and PV modules and a comparison to a standard side-by-side system.

Two configurations of the PVT system design are shown in Figure 7. Figure 7a shows a standard Domestic Hot Water system, which is the most installed solar thermal system in the Netherlands. Figure 7b shows a combination of a PVT system with a heat pump.
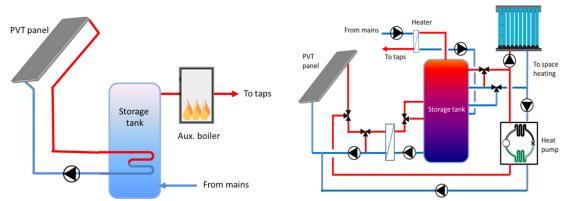

Figure 7 System designs used for simulations for PVT and solar thermal collectors. a) Simple DHW system b) parallel single-source solar heat pump

At the moment of writing, the detailed results are not yet available for publications. The trend of the suitability to fulfill a certain heat demand of the different systems is shown in Table 2.

	Regenerate ground source	DHW system	Source for heat pump
System A	++	--	?
System B	++	--	?
System C	++	+-	?

5. Conclusions

There is a large difference between the measured thermal performance of the three different collectors. These differences can be explained by the PVT collector design:

• The absorption factors of all PVT modules are quite good (0.9 – 0.94).

• A good heat conduction from the PV cells to the absorber leads to a high peak collector efficiency

• Insulation at the back of the PVT module improves the performance at higher temperatures.

PVT collector C performs the best, since it has a good heat conduction and insulation at the back. However, for systems that need low temperature heat, the other systems also can supply heat. Furthermore, the performance of some collectors can be improved by e.g. heat conducting paste, however, this may not lead to a techno-financial optimal solution.

System simulations with PVT as part of a solar heating system are carried out in TRNSYS and will yield valuable information on the annual yield for a specific system.

REFERENCES

[1] Zondag, H.A., Flat-plate PV-thermal collectors and systems: a review, Renewable and Sustainable Energy Reviews 12 (4) (2008) 891–959

[2] EN ISO 9806, Solar energy - Solar thermal collectors - Test methods (ISO 9806:2013)

Acknowledgements